Supporting Information for "A comprehensive picture for binary interactions of subaqueous barchans"

W. R. Assis[1], E. M. Franklin[2]

[1,2]School of Mechanical Engineering, UNICAMP - University of Campinas,

Rua Mendeleyev, 200, Campinas, SP, Brazil

Contents of this file

1. Figures S1 to S16

Additional Supporting Information (Files uploaded separately)

1. Captions for Movies S1 to S10

Introduction

This supporting information presents the layout of the experimental device, a photograph of the test section, microscopy images of the used grains, lists the tested conditions, snapshots of barchan interactions with different initial conditions and grain types, and movies showing examples of each collision pattern. We note that all individual images that were processed to plot Figures 3e and 3f of the paper and Figure S14 of this SI are available on Mendeley Data (http://dx.doi.org/10.17632/jn3kt83hzh.1).

The experiments described in the paper were conducted in a water channel of transparent material, for which the layout and a photograph of the test section are shown in Figs. S1 and S2, respectively. With the channel previously filled with water, controlled grains were poured inside, forming a pair of bedforms in either aligned or off-centered configurations. By imposing a water flow, each bedform was deformed into a barchan shape and interacted with each other.

A camera of complementary metal-oxide-semiconductor (CMOS) type was placed above the channel in order to acquire images of the bedforms. The camera resolution was of 1920 px $\times$ 1080 px at 60 Hz and it was mounted on a traveling system, both controlled by a computer. Depending on the tested conditions, the region of interest (ROI) was set to 1920 px $\times$ 701 px or to 1920 px $\times$ 801 px, and the frequency to 30 Hz. We used a lens of 60 mm focal distance and F2.8 maximum aperture mounted on the camera, and lamps of light emission diode (LED) were branched to a continuous-current source to provide the necessary light. The conversion from px to a physical system of units was made by means of a scale placed in the channel previously filled with water. The acquired images were processed by numerical scripts written in the course of this work. They basically removed the image background, binarized the images, and identified the main morphological properties of barchans and their relative distances.

Two observations are made just below concerning imperfections in our data.

OBS1: in Fig.S15 (below), test runs 1, 2, 3, 29, 33, 34 and 37 were in the frontier between the exchange and merging patterns, the resulting quantity of ejected grains being so small that the ejected bedform spread out as soon as it was ejected. We classified these experimental points as exchange, but we understand that they could be classified as merging as well.

OBS2: in Fig.S15 (below), the image recordings of test runs 24 and 44 were interrupted just before the end of the interaction process between barchans. This happened because the translation mechanism arrived at its end position. However, we observed that in both cases the interaction pattern was the fragmentation-chasing one (which can also be guessed from the respective movies).

Movie S1. Chasing_Alig.gif Movie showing an example of the chasing pattern in aligned configuration

Movie S2. Chasing_Stag.gif Movie showing an example of the chasing pattern in off-centered configuration

Movie S3. Merging_Alig.gif Movie showing an example of the merging pattern in aligned configuration

Movie S4. Merging_Stag.gif Movie showing an example of the merging pattern in off-centered configuration

Movie S5. Exchange_Alig.gif Movie showing an example of the exchange pattern in aligned configuration

Movie S6. Exchange_Stag.gif Movie showing an example of the exchange pattern in off-centered configuration

Movie S7. Fragmentation_Chasing_Alig.gif Movie showing an example of the fragmentation-chasing pattern in aligned configuration

Movie S8. Fragmentation_Chasing_Stag.gif Movie showing an example of the fragmentation-chasing pattern in off-centered configuration

Movie S9. Fragmentation_Exchange_Alig.gif Movie showing an example of the fragmentation-exchange pattern in aligned configuration

Movie S10. Fragmentation_Exchange_Stag.gif Movie showing an example of the fragmentation-exchange pattern in off-centered configuration

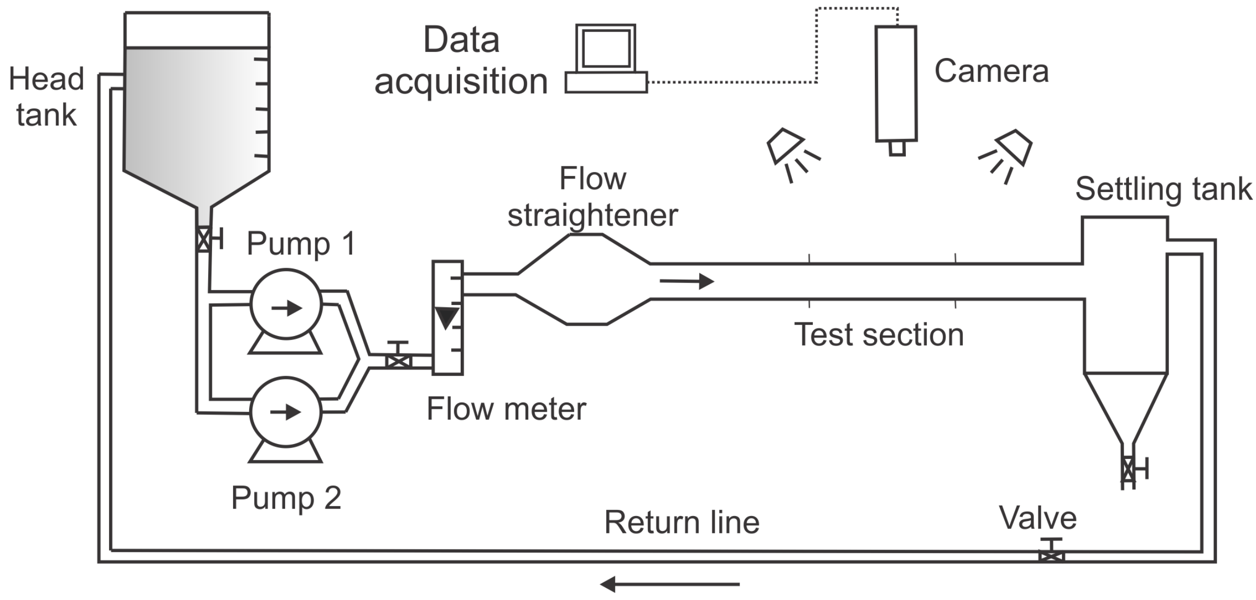

Figure S1. Layout of the experimental setup.

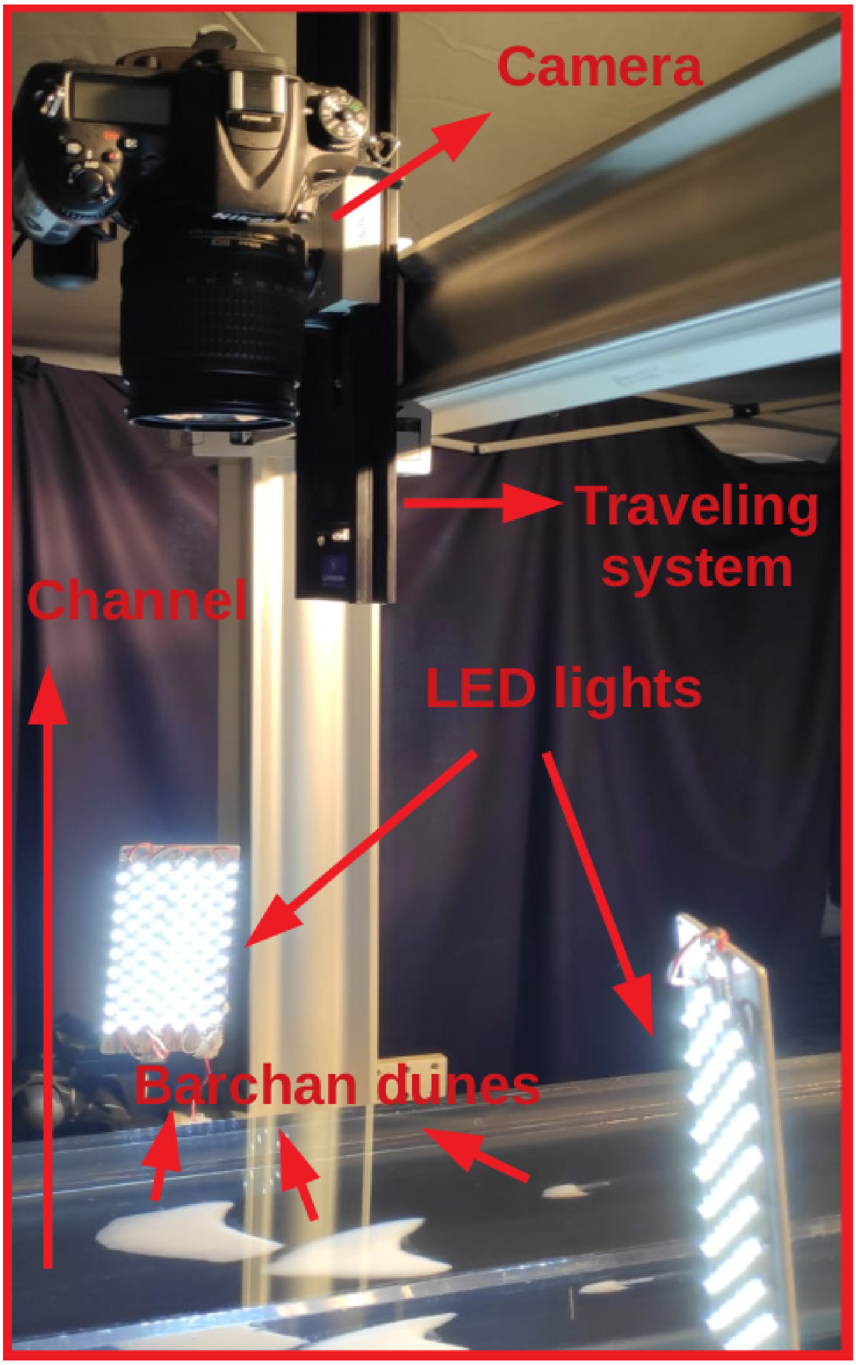

Figure S2. Photograph of the test section.

Figure S3. Microscopy image for the 0.40 mm $\leq d \leq$ 0.60 mm round glass beads of white color.

Figure S4. Microscopy image for the 0.40 mm $\leq d \leq$ 0.60 mm round glass beads of red color.

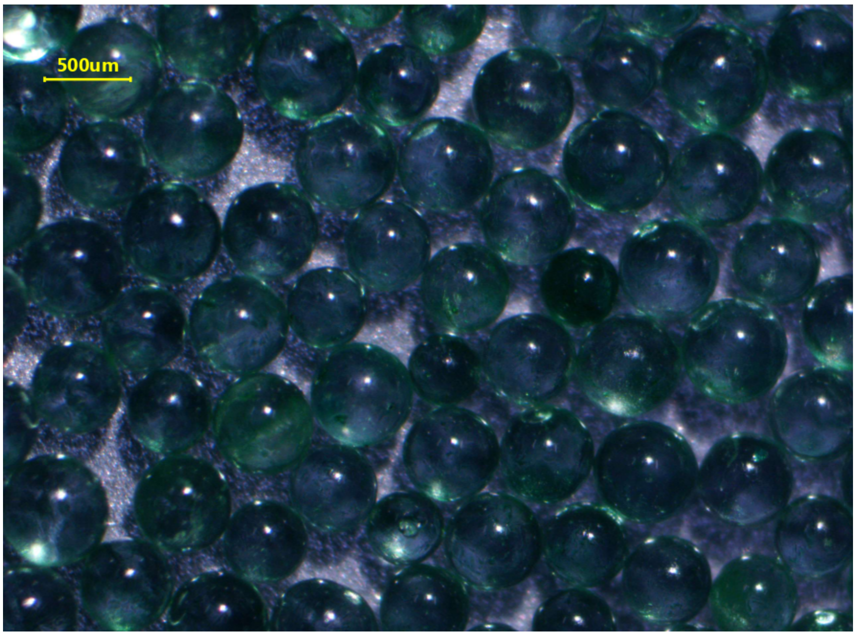

Figure S5. Microscopy image for the 0.40 mm $\leq d \leq$ 0.60 mm round glass beads of green color.

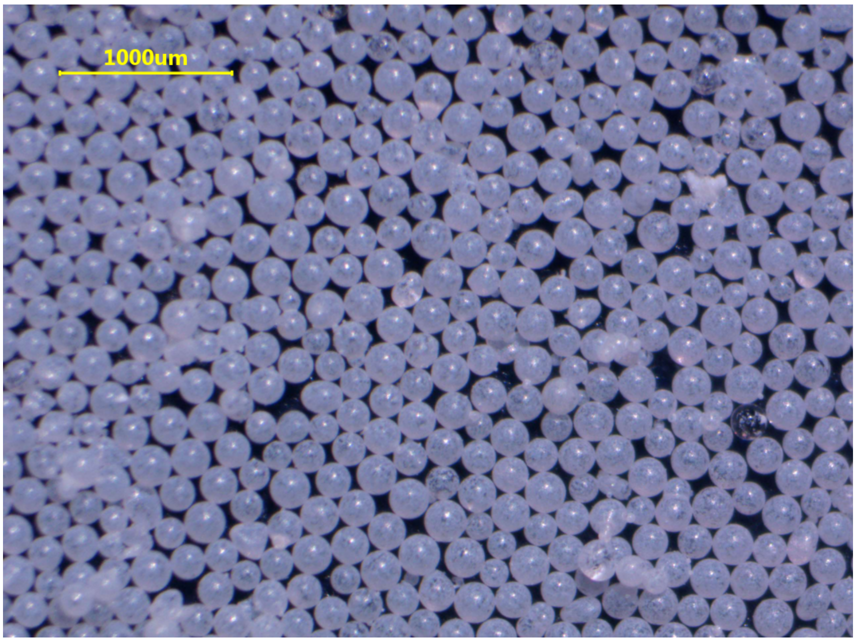

Figure S6. Microscopy image for the 0.15 mm $\leq d \leq$ 0.25 mm round glass beads of white color.

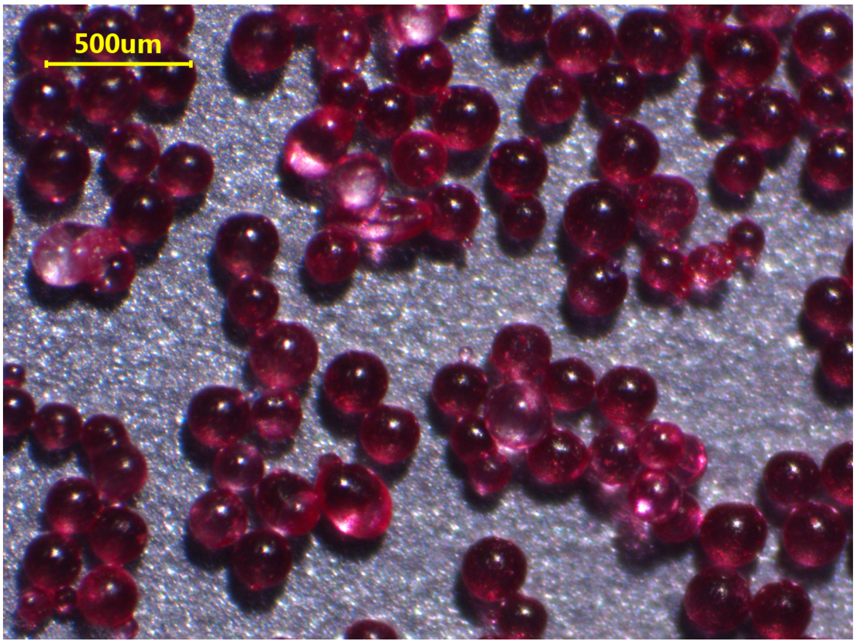

Figure S7. Microscopy image for the 0.15 mm $\leq d \leq$ 0.25 mm round glass beads of red color.

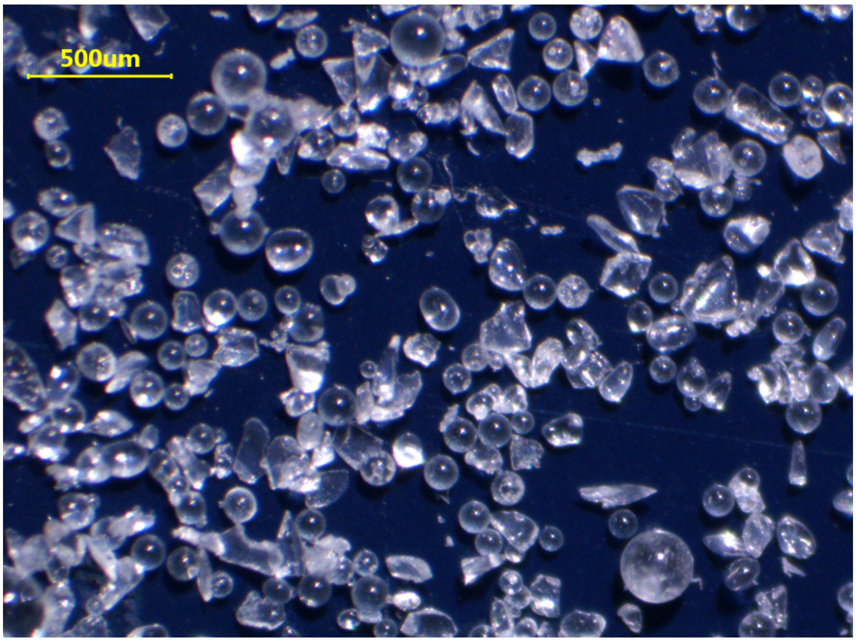

Figure S8. Microscopy image for the 0.21 mm $\leq d \leq$ 0.30 mm angular glass beads

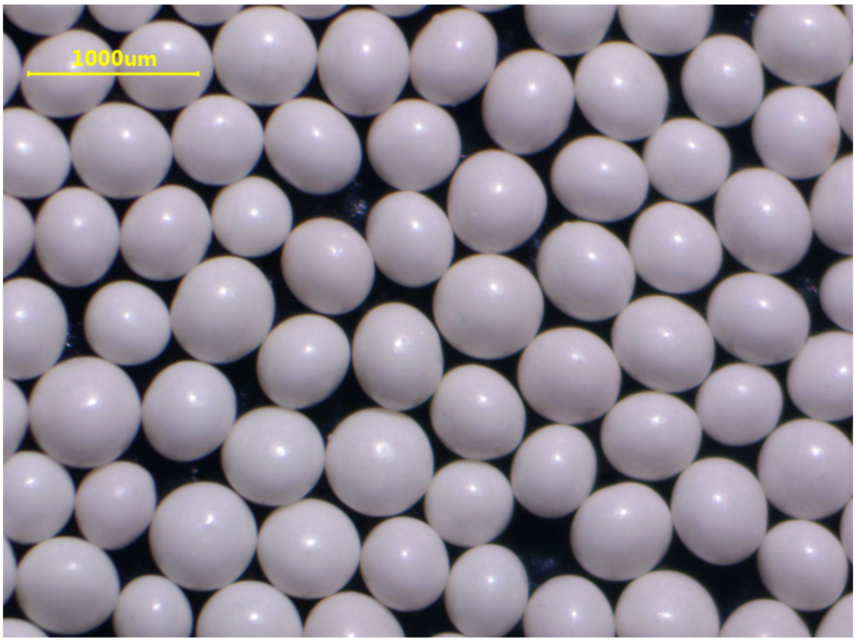

Figure S9. Microscopy image for the 0.40 mm $\leq d \leq$ 0.60 mm round zirconia beads.

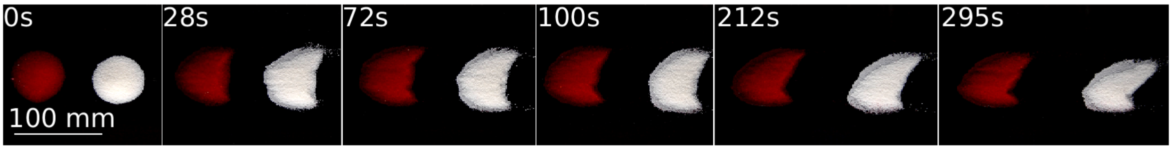

(a)

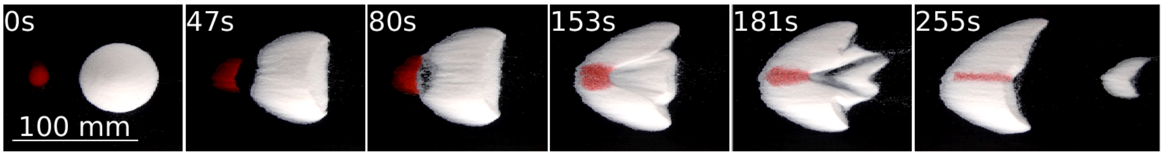

(b)

Figure S10. Snapshots of barchan interactions for aligned dunes, with two conical piles as initial condition. In the snapshots, the water flow is from left to right, the upstream pile consisting of red (darker) glass beads and the larger downstream pile of white (clearer) glass beads. In Fig. (a), 0.40 mm $\leq d \leq$ 0.60 mm, in Fig. (b) 0.15 mm $\leq d \leq$ 0.25 mm, and the corresponding times are shown in each frame. (a) Chasing; (b) exchange

(a)

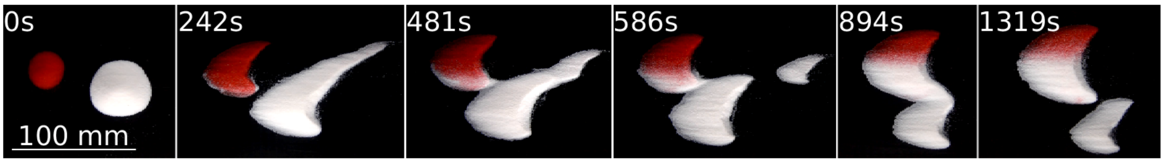

(b)

Figure S11. Snapshots of barchan interactions for off-centered dunes, with two conical piles as initial condition. In the snapshots, the water flow is from left to right, the upstream pile consisting of red (darker) glass beads and the larger downstream pile of white (clearer) glass beads. In Fig. (a), 0.40 mm $\leq d \leq$ 0.60 mm, in Fig. (b) 0.15 mm $\leq d \leq$ 0.25 mm, and the corresponding times are shown in each frame. (a) Merging; (b) fragmentation-exchange

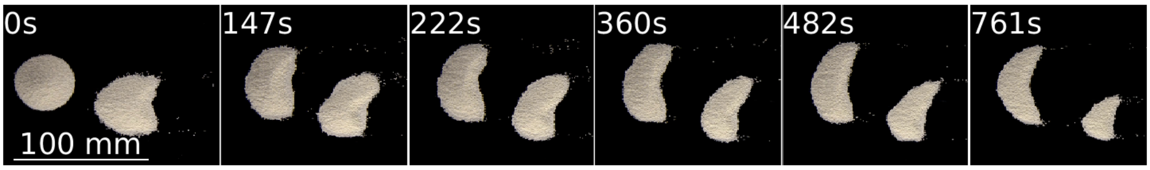

(a)

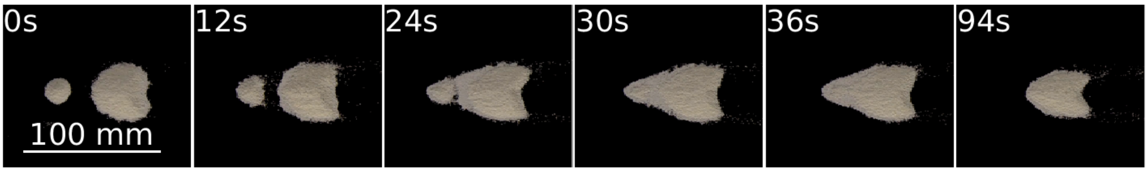

(b)

Figure S12. Snapshots of barchan interactions for off-centered and aligned dunes consisting of zirconium beads with 0.40 mm $\leq$ d $\leq$ 0.60. In the snapshots, the water flow is from left to right, and the corresponding times are shown in each frame. (a) Chasing (off-centered); (b) merging (aligned)

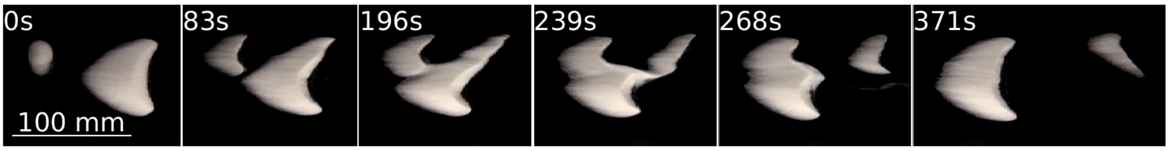

(a)

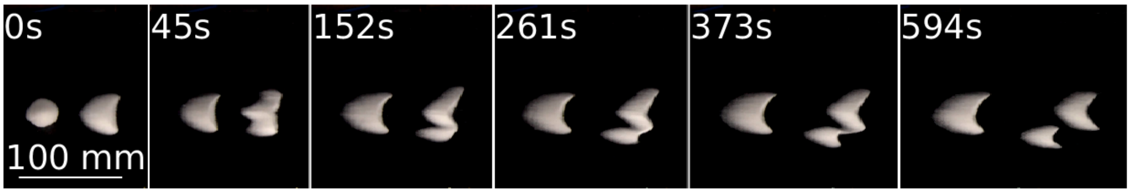

(b)

Figure S13. Snapshots of barchan interactions for off-centered and aligned dunes consisting of angular glass beads beads with 0.21 mm $\leq d \leq$ 0.30 mm. In the snapshots, the water flow is from left to right, and the corresponding times are shown in each frame. (a) Exchange (off-centered); (b) fragmentation-chasing (aligned)

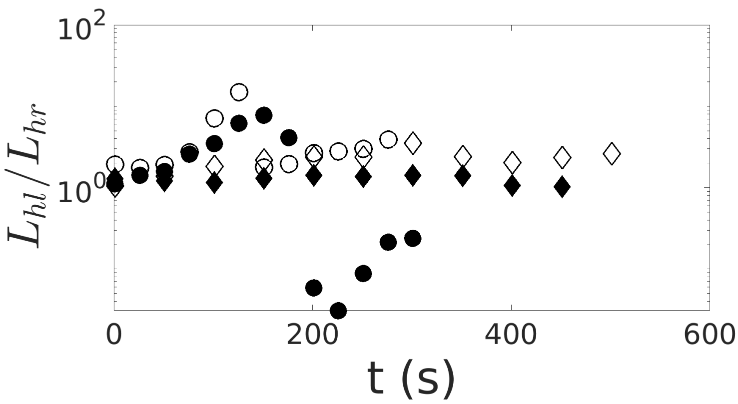

Figure S14. Ratio between the lengths of the left and right horns, L_{hl}/L_{hr}, of the downstream dune along time. Diamonds and circles correspond to the merging and exchange patterns, respectively. In both graphics, open symbols correspond to the aligned and solid symbols to off-centered cases.

Aligned position												
#	η(mm)	m_i(g)	m_t(g)	N_i	N_t	ξ_N	ρ_s(kg/m3)	d(mm)	u_*(m/s)	Re_*	θ	Pattern
1	0	2.0	8.0	12223	48892	0.6	2500	0.50	0.0141	7	0.027	Exchange
2	0	2.0	8.0	12223	48892	0.6	2500	0.50	0,0150	8	0.031	Exchange
3	0	2.0	8.0	12223	48892	0.6	2500	0.50	0.0159	8	0.034	Exchange
4	0	2.0	8.0	190986	763944	0.6	2500	0.20	0.0141	3	0.068	Fragmentation-Chasing
5	0	2.0	8.0	190986	763944	0.6	2500	0.20	0.0159	3	0.086	Fragmentation-Chasing
6	0	2.0	8.0	91069	364277	0.6	2500	0.26	0.0141	4	0.053	Fragmentation-Chasing
7	0	2.0	8.0	91069	364277	0.6	2500	0.26	0.0168	4	0.075	Fragmentation-Chasing
8	0	2.0	8.0	7453	29812	0.6	4100	0.50	0.0168	8	0.019	Merging
9	0	2.0	8.0	7453	29812	0.6	4100	0.50	0.0185	9	0.022	Merging
10	0	2.0	8.0	7453	29812	0.6	4100	0.50	0.0202	10	0.026	Merging
11	0	4.0	8.0	24446	48892	0.3	2500	0.50	0.0141	7	0.027	Fragmentation-Chasing
12	0	4.0	8.0	24446	48892	0.3	2500	0.50	0.0159	8	0.034	Fragmentation-Exchange
13	0	4.0	8.0	381972	763944	0.3	2500	0.20	0.0141	3	0.068	Fragmentation-Chasing
14	0	4.0	8.0	381972	763944	0.3	2500	0.20	0.0159	3	0.086	Fragmentation-Chasing
15	0	4.0	8.0	182138	364277	0.3	2500	0.26	0.0141	4	0.053	Fragmentation-Chasing
16	0	4.0	8.0	182138	364277	0.3	2500	0.26	0.0159	4	0.067	Fragmentation-Chasing
17	0	4.0	8.0	14906	29812	0.3	4100	0.50	0.0168	8	0.019	Merging
18	0	4.0	8.0	14906	29812	0.3	4100	0.50	0.0185	9	0.022	Merging
19	0	8.0	16.0	29812	59624	0.3	4100	0.50	0.0185	9	0.022	Merging
20	0	1.0	8.0	6112	48892	0.8	2500	0.50	0.0141	7	0.027	Merging
21	0	1.0	8.0	6112	48892	0.8	2500	0.50	0.0159	8	0.034	Merging
22	0	1.0	8.0	95493	763944	0.8	2500	0.20	0.0141	3	0.068	Fragmentation-Exchange
23	0	1.0	8.0	95493	763944	0.8	2500	0.20	0.0159	3	0.086	Fragmentation-Chasing
24	0	1.0	8.0	95493	763944	0.8	2500	0.20	0.0168	3	0.096	Fragmentation-Exchange
25	0	1.0	8.0	45535	364277	0.8	2500	0.26	0.0141	4	0.053	Fragmentation-Exchange
26	0	1.0	8.0	3727	29812	0.8	4100	0.50	0.0185	9	0.022	Merging
27	0	1.0	8.0	3727	29812	0.8	4100	0.50	0.0202	10	0.027	Merging
28	0	3.0	8.0	18335	48892	0.5	2500	0.50	0.0141	7	0.027	Merging
29	0	3.0	8.0	18335	48892	0.5	2500	0.50	0.0159	8	0.034	Exchange
30	0	0.3	14.0	1833	85562	1.0	2500	0.50	0.0141	7	0.027	Merging
31	0	0.1	3.0	9549	286479	0.9	2500	0.20	0.0141	3	0.068	Merging
32	0	0.1	3.0	9549	286479	0.9	2500	0.20	0.0159	3	0.086	Merging
33	0	0.3	14.0	28648	1336902	1.0	2500	0.20	0.0141	3	0.068	Exchange
34	0	0.3	8.0	28648	763944	0.9	2500	0.20	0.0141	3	0.068	Exchange
35	0	0.3	4.0	28648	381972	0.9	2500	0.20	0.0141	3	0.068	Exchange
36	0	0.3	14.0	28648	1336902	1.0	2500	0.20	0.0159	3	0.086	Exchange
37	0	0.3	14.0	13660	637484	1.0	2500	0.26	0.0141	4	0.053	Exchange
38	0	2.0	16.0	12223	97785	0.8	2500	0.50	0.0141	7	0.027	Exchange
39	0	3.0	20.0	18335	122231	0.7	2500	0.50	0.0141	7	0.027	Exchange
40	0	3.0	18.0	286479	1718873	0.7	2500	0.20	0.0141	3	0.068	Fragmentation-Exchange
41	0	12.0	16.0	44719	59624	0.1	4100	0.50	0.0185	9	0.022	Merging
42	0	0.5	6.0	47746	572958	0.8	2500	0.20	0.0159	3	0.086	Fragmentation-Exchange
43	0	0.3	6.0	28648	572958	0.9	2500	0.20	0.0159	3	0.086	Exchange
44	0	0.3	6.0	13660	273208	0.9	2500	0.26	0.0141	4	0.053	Exchange
45	0	0.1	20.0	4553	910692	1.0	2500	0.26	0.0141	4	0.053	Merging
46	0	1.5	2.0	68302	91069	0.1	2500	0.26	0.0141	4	0.053	Fragmentation-Chasing
47	0	3.0	3.0	136604	136604	0.0	2500	0.26	0.0141	4	0.053	Fragmentation-Chasing
48	0	1.5	4.0	68302	182138	0.5	2500	0.26	0.0159	4	0.067	Fragmentation-Chasing
49	0	2.0	4.0	12223	24446	0.3	2500	0.50	0.0133	7	0.024	Merging
50	0	0.6	8.0	3667	48892	0.9	2500	0.50	0.0141	7	0.027	Merging
51	0	0.7	12.0	2609	44719	0.9	4100	0.50	0.0185	9	0.022	Merging
52	0	1.5	2.0	143239	190986	0.1	2500	0.20	0.0141	3	0.068	Fragmentation-Chasing
53	0	3.0	3.0	286479	286479	0.0	2500	0.20	0.0159	3	0.086	Chasing
54	0	9.0	10.0	33539	37266	0.1	4100	0.50	0.0202	10	0.027	Chasing
55	0	10.0	10.0	61115	61115	0.0	2500	0.50	0.0141	7	0.027	Chasing
56	0	9.0	10.0	55004	61115	0.1	2500	0.50	0.0159	8	0.034	Exchange
57	0	2.7	3.0	257831	286479	0.1	2500	0.20	0.0141	3	0.068	Fragmentation-Chasing
58	0	2.7	3.0	257831	286479	0.1	2500	0.20	0.0159	3	0.086	Chasing
59	0	3.0	3.0	286479	286479	0.0	2500	0.20	0.0141	3	0.068	Fragmentation-Chasing
60	0	2.7	3.0	16501	18335	0.1	2500	0.50	0.0159	8	0.034	Chasing
61	0	3.0	3.0	18335	18335	0.0	2500	0.50	0.0159	8	0.034	Chasing
62	0	6.0	8.0	36669	48892	0.1	2500	0.50	0.0159	8	0.034	Fragmentation-Chasing
63	0	3.0	3.0	136604	136604	0.0	2500	0.26	0.0141	4	0.053	Fragmentation-Chasing
64	0	2.7	3.0	122943	136604	0.1	2500	0.26	0.0141	4	0.053	Fragmentation-Chasing

Figure S15. List of the tested conditions in the aligned configuration. η is the offset distance between the centroids, m_i and m_t are the masses of the impacting (upstream) and target (downstream) dunes, respectively, N_i and N_t are the number of grains of the impacting and target dunes, respectively, ξ_N is the dimensionless particle number, ρ_s and d are the density and mean diameter of grains, respectively, u_* is the shear velocity, Re_* is the particle Reynolds number, θ is the Shields number, and *Pattern* corresponds to the collision pattern.

Off-centered position													
#	η(mm)	σ	m_i(g)	m_t(g)	N_i	N_t	ξ_N	ρ_s(kg/m3)	d(mm)	u_*(m/s)	Re_*	θ	Pattern
1	22	0.5	2.0	8.0	12223	48892	0.6	2500	0.50	0.0141	7	0.027	Merging
2	28	0.7	2.0	8.0	12223	48892	0.6	2500	0.50	0.0150	8	0.031	Merging
3	25	0.6	2.0	8.0	12223	48892	0.6	2500	0.50	0.0159	8	0.034	Merging
4	26	0.6	2.0	8.0	190986	763944	0.6	2500	0.20	0.0141	3	0.068	Fragmentation-Exchange
5	18	0.4	2.0	8.0	190986	763944	0.6	2500	0.20	0.0159	3	0.086	Fragmentation-Exchange
6	16	0.4	2.0	8.0	7453	29812	0.6	4100	0.50	0.0168	8	0.019	Merging
7	17	0.5	2.0	8.0	7453	29812	0.6	4100	0.50	0.0202	10	0.027	Merging
8	25	0.5	4.0	8.0	24446	48892	0.3	2500	0.50	0.0141	7	0.027	Chasing
9	22	0.5	4.0	8.0	24446	48892	0.3	2500	0.50	0.0159	8	0.034	Chasing
10	24	0.5	4.0	8.0	381972	763944	0.3	2500	0.20	0.0141	3	0.068	Chasing
11	27	0.6	4.0	8.0	381972	763944	0.3	2500	0.20	0.0159	3	0.086	Fragmentation-Chasing
12	16	0.4	4.0	8.0	14906	29812	0.3	4100	0.50	0.0168	8	0.019	Chasing
13	15	0.4	4.0	8.0	14906	29812	0.3	4100	0.50	0.0202	10	0.027	Merging
14	24	0.6	1.0	8.0	6112	48892	0.8	2500	0.50	0.0141	7	0.027	Merging
15	22	0.5	1.0	8.0	6112	48892	0.8	2500	0.50	0.0159	8	0.034	Merging
16	21	0.5	1.0	8.0	95493	763944	0.8	2500	0.20	0.0141	3	0.068	Exchange
17	21	0.5	1.0	8.0	95493	763944	0.8	2500	0.20	0.0159	3	0.086	Exchange
18	18	0.4	1.0	8.0	45535	364277	0.8	2500	0.26	0.0159	4	0.067	Exchange
19	14	0.4	1.0	8.0	3727	29812	0.8	4100	0.50	0.0168	8	0.019	Merging
20	16	0.5	1.0	8.0	3727	29812	0.8	4100	0.50	0.0202	10	0.027	Merging
21	26	0.6	3.0	8.0	18336	48892	0.5	2500	0.50	0.0141	7	0.027	Chasing
22	23	0.5	3.0	8.0	18336	48892	0.5	2500	0.50	0.0159	8	0.034	Merging
23	19	0.4	3.0	8.0	136604	364277	0.5	2500	0.26	0.0141	4	0.053	Fragmentation-Exchange
24	19	0.4	3.0	8.0	286479	763944	0.5	2500	0.20	0.0159	3	0.086	Fragmentation-Chasing
25	19	0.4	3.0	8.0	286479	763944	0.5	2500	0.20	0.0176	4	0.106	Fragmentation-Chasing
26	15	0.4	3.0	8.0	11181	29812	0.5	4100	0.50	0.0168	8	0.019	Merging
27	16	0.4	3.0	8.0	11181	29812	0.5	4100	0.50	0.0202	10	0.027	Merging
28	22	0.4	6.0	8.0	36669	48892	0.1	2500	0.50	0.0141	7	0.027	Chasing
29	17	0.3	6.0	8.0	36669	48892	0.1	2500	0.50	0.0159	8	0.034	Chasing
30	20	0.4	6.0	8.0	572958	763944	0.1	2500	0.20	0.0141	3	0.068	Chasing
31	21	0.4	6.0	8.0	572958	763944	0.1	2500	0.20	0.0159	3	0.086	Fragmentation-Chasing
32	16	0.4	6.0	8.0	22359	29812	0.1	4100	0.50	0.0168	8	0.019	Chasing
33	15	0.4	6.0	8.0	22359	29812	0.1	4100	0.50	0.0202	10	0.027	Chasing
34	32	0.7	0.3	14.0	1833	85562	1.0	2500	0.50	0.0141	7	0.027	Merging
35	20	0.5	0.3	14.0	1833	85562	1.0	2500	0.50	0.0159	8	0.034	Merging
36	22	0.5	0.3	14.0	28648	1336902	1.0	2500	0.20	0.0141	3	0.068	Exchange
37	24	0.5	0.3	14.0	28648	1336902	1.0	2500	0.20	0.0159	3	0.086	Exchange
38	20	0.4	0.1	20.0	9549	1909859	1.0	2500	0.20	0.0141	3	0.068	Merging
39	17	0.4	0.1	20.0	9549	1909859	1.0	2500	0.20	0.0159	3	0.086	Exchange
40	15	0.4	0.5	6.0	47746	572958	0.8	2500	0.20	0.0141	3	0.068	Exchange
41	13	0.4	0.5	6.0	47746	572958	0.8	2500	0.20	0.0159	3	0.086	Exchange
42	19	0.5	3.0	3.0	286479	286479	0.0	2500	0.20	0.0141	3	0.068	Chasing
43	15	0.4	3.0	3.0	286479	286479	0.0	2500	0.20	0.0159	3	0.086	Chasing
44	14	0.3	3.0	3.0	136604	136604	0.0	2500	0.26	0.0141	4	0.053	Fragmentation-Chasing
45	20	0.3	10.0	10.0	61115	61115	0.0	2500	0.50	0.0141	7	0.027	Chasing
46	20	0.3	10.0	10.0	61115	61115	0.0	2500	0.50	0.0159	8	0.034	Chasing
47	17	0.4	8.0	8.0	29812	29812	0.0	4100	0.50	0.0168	8	0.019	Chasing
48	16	0.4	8.0	8.0	29812	29812	0.0	4100	0.50	0.0202	10	0.027	Chasing

Figure S16. List of the tested conditions in the off-centered configuration. η is the offset distance between the centroids, σ is the offset parameter, m_i and m_t are the masses of the impacting (upstream) and target (downstream) dunes, respectively, N_i and N_t are the number of grains of the impacting and target dunes, respectively, ξ_N is the dimensionless particle number, ρ_s and d are the density and mean diameter of grains, respectively, u_* is the shear velocity, Re_* is the particle Reynolds number, θ is the Shields number, and *Pattern* corresponds to the collision pattern.